Probing Molecular Dynamics by Femtosecond Time-Resolved Coherent Anti Stokes Raman Spectroscopy

M Schmitt[1], T Siebert[1], A S Grabtchikov[2], V. Orlovich[2], and W Kiefer[1]

[1]*Institut für Physikalische Chemie, Universität Würzburg,*
Am Hubland, D-97074 Würzburg, Federal Republic of Germany
[2]*B. I. Stepanov Institute of Physics, National Academy of Sciences of Belarus, Minsk, Belarus*

Femtosecond time-resolved CARS spectroscopy is applied in order to prepare and monitor coherent states of different samples. The time evolution prepared by such methods gives information on the dynamics of molecular vibrations. In a first example the electronic ground state dynamics of biologically relevant porphyrin molecules are studied with transient CARS spectroscopy. Second, we report on selective excitation of the vibrational modes in the electronic ground state of polymers of diacetylene by means of a femtosecond time-resolved CARS scheme. Control is achieved by varying the timing and the phase shape (chirp) of the exciting laser pulses. Finally the capability of the CARS process to interrogate individual normal modes was utilised for exploring the influence of nuclear dynamics on the process of the S_1/S_0 internal conversion (IC) in β-carotene, by placing the CARS process in a *pump-probe* scheme, where it plays the role of a mode selective probe.

1 INTRODUCTION

Elementary steps in chemical reactions involve the breaking and formation of molecular bonds. The time-scale for these processes is on the order of 100 fs. Therefore, femtosecond time-resolved spectroscopy enables researchers to have a direct view of the ultrafast dynamics taking place in molecules after coherent excitation[1,2]. Femtosecond (fs) time-resolved spectroscopy has evolved into a highly diverse research field over the last decade which has opened up new exciting possibilities for the investigation of chemical processes directly on the time scale of the fastest elementary steps[1-6]. Ultrashort laser pulses with a duration of less than about 100 femtoseconds allow for a coherent broadband excitation with preparation and detection of rotational and vibrational superposition states. The time-evolution of these rovibrational wave packets on the potential energy surfaces (PES) gives information on the molecular dynamics. However, despite the great variety of experimental techniques that has been developed[1-6], there are only few methods that are capable to study ultrafast molecular dynamics in the electronic ground state[7-14], one of which is the method of fs time-resolved four-wave mixing (FWM) spectroscopy[15-26]. Especially for more-complex molecular systems it is interesting to gain information about the ground state dynamics.

In the present contribution, we review some of the work on femtosecond time-resolved FWM spectroscopy recently performed in our laboratories[27-36]. We would like to point out the main advantages of this technique and to emphasize its capability for investigating ground state dynamics. We have demonstrated that by the CARS method one can observe the dynamics of a wave packet either evolving on the ground or an excited state PES[31,37-47]. The dynamics which shows itself in the CARS transient depends on the relative timing of the three laser pulses giving rise to the nonlinear FWM process. Next to the timing of the laser pulses there are other degrees of freedom which can be varied in order to gain even more information on the ultrafast ro-vibrational dynamics evolving in the excited molecules.

The following points will be discussed below: first, we introduce the general methodology employed in experiments for a KGW single crystal ($KGd(WO_4)_2$). Second, we demonstrate that also for more complex molecules (polydiacetylenes, porphyrins and β-carotene) mode dynamics are accessible making use of the spectral components of the transient FWM signal.

2 EXPERIMENTAL

The experimental apparatus has been described in detail elsewhere[37,41,48]. Briefly, for the porphyrin experiments a 1 kHz Ti:sapphire femtosecond laser system in combination with three four pass OPAs were used to create up to three femtosecond pulses simultaneously. The pulses had energies of a few μJ and pulse durations of typically 80 fs. For the solid state experiments on KGW and PDAs and the condensed phase experiments on β-carotene the laser system consisted of a Ti:sapphire oscillator and a regenerative amplifier pumping two white light OPAs . At the output of the regenerative amplifier the pulses at 800 nm have a repetition rate of 100 kHz. The white-light OPAs generate ≈ 100 fs pulses in the range 480-700 nm, with an energy per pulse of approximately 100 nJ. In all experiments, one of the OPA outputs is branched by a 1:1 beam splitter to produce two of the laser pulses at the same wavelength. The output of the second OPA is used as a third laser pulse. The *initial pump* laser at 400 nm needed for the *pump* CARS experiments on β-carotene described in section 3.3 was produced using the residual second harmonic light produced in one of the OPAs. The laser pulses can be delayed in time relative to each other by means of Michelson-interferometer arrangements. As a spatial beam geometry for the FWM measurements we have used the folded BOX-CARS configuration[49]. The four involved light beams are spatially separated in this arrangement, allowing for a background free detection of the signal. Furthermore the phase matching condition is fulfilled. The FWM signal was spectrally filtered with the help of a monochromator and detected by a CCD camera (Photometrics). The broadband detection with a CCD camera offers many advantages as the whole spectral range of the FWM signal can be resolved for each pulse (see results and discussion).

In this paper, we present results on femtosecond time-resolved CARS investigations of a KGW single crystal, porphyrins, polymers of diacetylenes embedded in diacetylene single crystals and β-carotene. The investigated porphyrine samples have been used as purchased (Porphyrin products). All measurements have been performed in solution, using a flow-type cuvette which has been built from a rectangular glass capillary (Vitro Dynamics Inc.). As solvent we chose dichloromethane, because it possesses only weak vibrational bands in the excitation region and is relatively inert and non-polar compared with other solvents. Sample concentrations have been adjusted to yield a linear absorption of typically 1.2 OD for the strongest Q-band in a 1 mm path length cuvette. The polydiacetylenes (PDAs) under consideration are TS6 (sidegroup: $-CH_2-O-SO_2-C_6H_4-CH_3$) and FBS (sidegroup: $-CH_2-O-SO_2-C_6H_4-F$)[50-51]. Both were prepared according to the method described by Wegner[50]. The crystals were cleaved parallel to the 100 surface (containing b- and c-axes) to produce thin platelets of about 100 μm thickness and about 3 mm length in the chain direction (|| b-axis). For the experiments, the crystals were cooled down in a closed cycle helium cryostate to a temperature of approximately 8 K. β-carotene has been used as purchased (Aldrich). All measurements have been performed on 0.1 mM solutions of β-carotene in *n*-hexane, using a rotating sample cell (100 Hz) with a cell length of 0.5 mm.

3 RESULTS AND DISCUSSION

In the following, we discuss experimental results of femtosecond time-resolved coherent anti-Stokes Raman (CARS) experiments on various different systems. We present results which give a flavor of the wide capabilities of the fs time-resolved CARS technique.

In a fs-CARS experiment two time coincident femtosecond laser pulses (*pu*, and *S*) and a third laser pulse (*pu$_{\Delta t}$*) delayed by Δt, coherently interact with the sample. The wavenumber difference between the *pump* (*pu*, *pu$_{\Delta t}$*) and the Stokes lasers (*S*) are chosen to be resonant with a vibrational transition within the ground state of the sample molecules. The time coincident pulses *pu* and *S* generate a coherent ground

state vibrational excitation. The *pump* pulse $pu_{\Delta t}$ follows the interaction of the two laser fields at $\Delta t = 0$ and acts as a probe of the response of the coherently excited molecules prepared by the coincident *pu* and *S* laser pulses.

3.1 KGd(WO₄)₂: Vibrational Dynamics in a simple System

In Fig 1 we show as an illustrating example the experimentally observed CARS intensity as a function of delay time Δt between the *pump* pulse $pu_{\Delta t}$ and the two time coincident pulses *pu* and *S* for a KGW single crystal (KGd(WO₄)₂). For the Raman excitation a wavenumber difference of $\Delta\tilde{v}_{pu} - \Delta\tilde{v}_{s} = 760$ cm^{-1} between the *pump* and the Stokes laser was chosen. As a result of the spectral width of the femtosecond exciting lasers of more than 200 cm^{-1}, several modes were coherently excited namely the Raman active vibrations of KGW at wavenumber positions 900, 766 and 685 cm^{-1}. The preparation of a vibrational wavepacket composed of several eigenstates for the vibrational degrees of freedom results in quantum beats in the CARS signal, as can be seen in Fig 1. The oscillations belong to the vibrational energy differences in the KGW crystal. To analyse the experimental data shown in Fig 1 we give the results of a fast Fourier transform (FFT) of the transient in the insert of Fig 1. The FFT spectrum shows three peaks which correspond to the wavenumber difference of the three coherently excited modes beating with each other. This two-photon process generating a coherent ground state vibrational excitation is highly flexible. The excitation energy in the electronic ground state can be adjusted by the energy difference of the *pump* and the Stokes photons, making this method perfectly suitable for the selective excitation and probing of vibrational dynamics. Furthermore, the excitation can also be performed resonantly via an excited electronic state. In this case an additional time-delay between the *pump* and the Stokes pulses might be introduced during which the generated amplitude by the *pump* pulse evolves unperturbed on the excited state potential energy surface. The method of time resolved CARS can be applied not only to gain time-resolved information on the investigated samples but also wavenumber-resolved information by varying the wavelength window which is opened for the detection of the CARS signal. In the following we demonstrate that for complex molecules (polydiacetylenes, porphyrins, β-carotene) mode dynamics are accessible making use of the wide capabilities of the CARS technique.
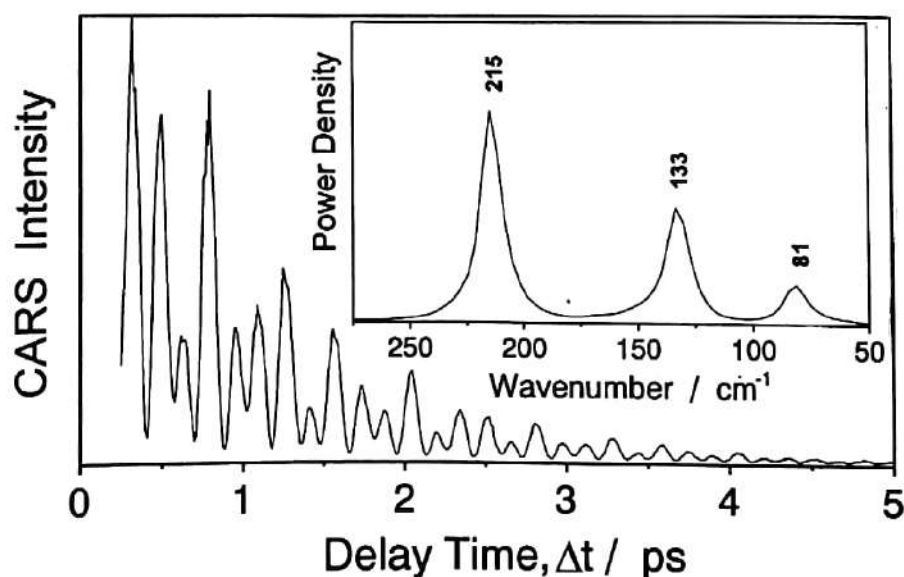

Figure 1   Femtosecond CARS transient taken of a KGW-crystal. The insert shows the result of a FFT of this transient[52].

3.2 Porphyrins: Vibrational Dynamics in Large Molecules

Next, we report on fs time-resolved CARS measurements to investigate the electronic ground state vibrational dynamics of large, biologically relevant molecules namely porphyrins. Porphyrins have attracted considerable attention in the last couple of years, because they form the active sites of many important biological systems such as hemoglobins, peroxidases or photoreaction centers. In this subsection fs CARS measurements performed on these biologically relevant porphyrin molecules are presented. The vibrational information which one wishes to extract from the transient CARS signal is often obscured by non-Raman resonant contributions. This is especially a problem, when like here the investigated molecular system is studied in solution: The decay of the resonant isotropic contribution, which corresponds to pure vibrational dynamics, occurs on a much faster timescale than in isolated molecules, and additionally, the nonresonant CARS signal from the solvent is often orders of magnitude higher than the signal from the system one intends to study. In order to overcome this problem we have applied one of the so-called magic polarization geometries[52], where by a special setting of the polarization directions of the incident pulses, and a proper analyzer polarization direction for the coherently scattered signal, the non-Raman resonant background is supressed.

Figure 2(A) shows a typical spectrally dispersed transient CARS signal as a function of Δt and the CARS wavenumber $\Delta \tilde{v}_{aS}$. It has been obtained from MgOEP dissolved in dichloromethane, for a *pump* pulse wavelength of 580 nm and a Stokes pulse wavelength of 631 nm. The signal is centered at about $\Delta \tilde{v}_{aS} = 1400$ cm^{-1}, corresponding to the mean excitation energy determined by the wavenumber difference of the *pump* and the Stokes laser. It extends from $\Delta \tilde{v}_{aS} \approx 1000$ cm^{-1} to $\Delta \tilde{v}_{aS} \approx 1800$ cm^{-1} and lasts for about 4 ps. Such a wavelength arrangement has been chosen to achieve a strong resonance enhancement of the CARS process via excited electronic states. The wavelengths of the *pump/probe* pulses have therefore been tuned to the absorption maximum of the Q_{00} band. Together with a Stokes pulse wavelength that is determined by the required excitation wavenumber to excite modes of the porphyrin macrocycle, this results in a wavelength of the CARS signal in the vicinity of the Q_{01} absorption band maximum.
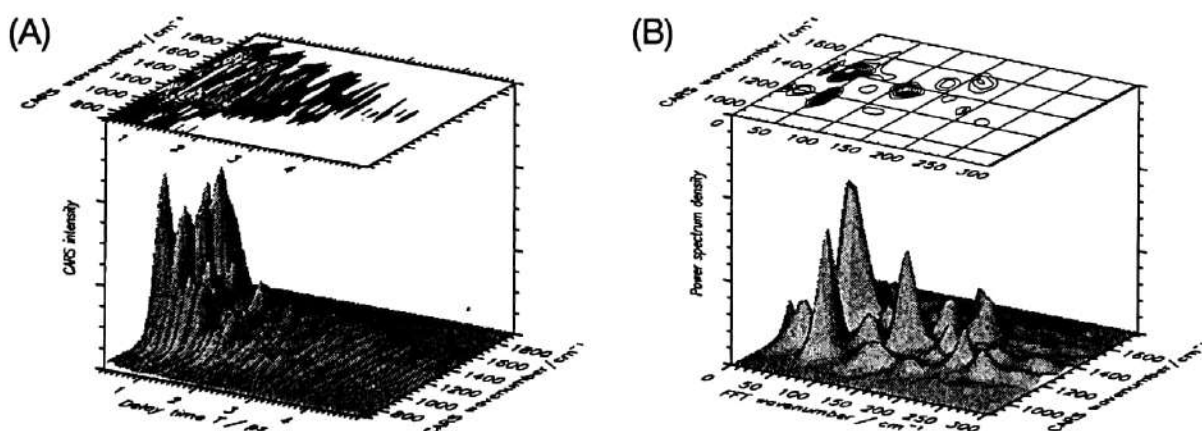

Figure 2   (A) Typical spectrally dispersed-detected fs-CARS signal for MgOEP dissolved in dichloromethane for an excitation wavenumber in the spectral region of the modes of the MgOEP macrocycle. (B) PSD of the transient CARS signal of MgOEP for an excitation wavenumber of 1350 cm^{-1}, indicating that a large number of modes is coherently excited in this measurement.

The signal shows the expected oscillatory pattern for the high density of coherently excited normal modes in the ground state of this system, with a strongly modulated structure in both, the direction of the time axis and the wavenumber axis.

To investigate this complex signal structure we employed Fourier transform methods and calculated the power spectrum density (PSD) at every spectral position $\Delta\tilde{v}_{as}$ of the time domain signal using the "Fast Fourier transformation method" (FFT). Except for a subtraction of the exponentially decaying component of the transient signal which retains only oscillatory components and therefore removes the low frequency component in the wavenumber domain data, no additional processing or smoothening of the data has been performed.

Figure2(B) shows a calculated PSD plot of a transient CARS signal where the mean excitation wavenumber is tuned to about 1350 cm^{-1} with a *pump/probe* pulse wavelength of 580 nm and a corresponding Stokes pulse wavelength of 629 nm. The excitation of a multitude of vibrational modes now leads to a strongly modulated transient signal. The PSD contains several strong and weak peaks. Recalling that the position of the peak along the CARS wavenumber axis is given approximately by the arithmetic mean wavenumber of two vibrational modes beating with each other and that the peak location along the FFT wavenumber axis corresponds to the wavenumber difference of the two modes, we can compare the peak position to the vibrational mode spectrum of MgOEP reported in the literature[54]. The complete assignment of the excited modes is given in Table 1. The assignment of these peaks to vibrational modes has been performed by a comparison of these results to data obtained from resonance Raman measurements and ns-CARS experiments[54,55]. To this end we took advantage of the fact that the FFT wavenumber position of the peaks in the PSD plots directly corresponds to the wavenumber difference $\Delta\tilde{v}_j - \Delta\tilde{v}_k$ of modes v_j and v_k. This information allows to derive spectral information on the relative peak positions of individual vibrational modes from these measurements.

Table 1: Vibrational modes contributing to the fs-CARS signal of MgOEP at a excitation wavenumbers of 1350 cm^{-1}.

$\Delta\tilde{v}_{FFT}$	$\Delta\tilde{v}_{as}$	v_k	$\Delta\tilde{v}_k$	v_j	$\Delta\tilde{v}_j$	$\Delta\tilde{v}_j - \Delta\tilde{v}_k$
cm^{-1}	cm^{-1}	assignment	cm^{-1}	assignment	cm^{-1}	cm^{-1}
10	1435	CH_2 scis	1434	CH_2 scis	1440	6
22	1210	v_{13} (b_{1g})	≈ 1210			
38	1435	v_{29} (b_{2g})	1400	CH_2 scis	1440	40
50	1200	v_{30} (b_{2g})	≈ 1160	v_{13} (b_{1g})	≈ 1210	≈ 50
110	1370	v_{21} (a_{2g})	1317	CH_2 scis	1434	117
140	1470	v_{29} (b_{2g})	1400	v_{19} (a_{2g})	1546	146
175	1520	v_{20} (a_{2g})	1387	v_{11} (b_{1g})	1552	165

3.3 Polydiacetylenes: Control of Mode Dynamics

The control of chemical reactions is one of the main goals of chemists. One way to achieve this goal is photochemistry where the energy to break bonds is added in form of light[56]. The absorption of light results in internal vibration as well as translational or rotational motion. When molecules are heated indiscriminately the energy will be distributed statistically among all degrees of freedom; no selectivity can be achieved, the weakest bonds will break first and therefore, only a limited set of reactions is possible. In this subsection we describe results for the possibility of selectively exciting specific vibrational modes in molecules which are characterized by multidimensional potential energy surfaces (PES). We demonstrate that by the application of fs time-resolved coherent anti-Stokes Raman scattering (CARS) we are able to selectively excite ground state vibrations and also detect the time response of these modes as well as neighboring modes. The experiments were performed on diacetylene single crystals containing less than 1% polymer molecules. For the polydiacetylenes (PDAs) there exist two different mesomeric structures of their backbones which can be described as äcetylene-type" $(=RC-C \equiv C-CR'=)_n$ and "butatriene-type" $(-RC=C=C=CR'-)n$. While the ground state of the considered PDAs (TS6 and FBS) is described by the acetylenic structure, the excitonic state is characterized by a geometric relaxation model. Pham *et al.*[57] assumed that the resonant optical excitation of the PDAs takes them to their free excitonic state (FE) from where a formation of self-trapped excitons (STE) takes place. FE and STE backbones have butatriene and acetylene type structure, respectively[58]. The laser wavelengths for the fs CARS experiment were chosen such that electronic as well as Raman resonances were met. The wavelengths of the two *pump* lasers were set to $\lambda_{pu_u} = \lambda_{pu} = 605$ nm which is close to resonance with the polymer absorption. The Stokes laser had a wavelength of $\lambda_S = 652$ nm in order to excite the vibrational modes in the ground state. These modes are v_2 (1475 cm^{-1}), $v_{2'}$ (1460 cm^{-1}), v_3 (1200 cm^{-1}) and v_4 (960 cm^{-1}) which involve C=C and C-C stretching and bending motions. The mode $v_{2'}$ is a side group CH_3 scissors vibration which is coupled to the v_2 mode by a Fermi resonance.
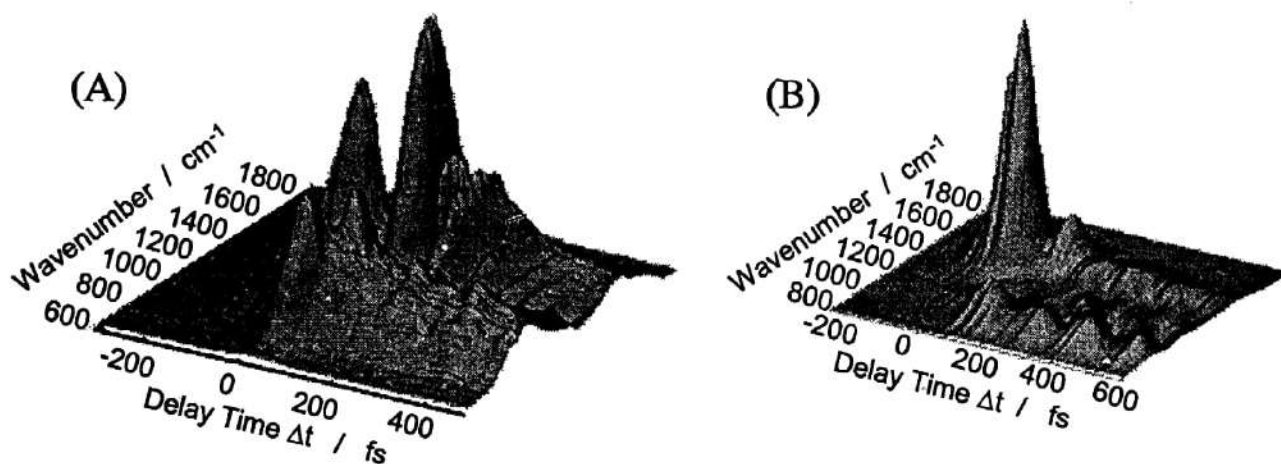

Figure 3 The influence of the excitation laser's chirp on the mode excitation; (A) minimal chirp; (B) laser chirp was introduced to selectively enhance $v_2 / v_{2'}$ contribution.

The general idea of the experiments discussed in the following was to optimize the excitation of different vibrational modes in the electronic ground state of the PDA molecules. This goal can be achieved by varying the time dependent phase of the exciting *pump* and/or Stokes lasers. The idea here is to use tailored femtosecond laser pulses by arranging the frequency components inherently belonging to an ultrashort laser pulse in a way that discriminates or enhances the excitation of selective normal modes. This can be achieved by amplitude and/or phase modulation of the ultrashort laser pulses. First, the chirp was minimized by compressing the pulses by means of a prism compressor to their transform limit of 70 fs in order to obtain a reference transient.

Panel (A) of Fig 3 shows this transient. All vibrational modes contribute which are excited by the spectrally broad *pump* and Stokes lasers (Raman resonance for the central wavenumbers with the v_3 mode was chosen). Adding some linear chirp by moving one of the compressor prisms of the exciting laser pulses, the behaviour can be changed dramatically. By tuning the position of one of the prisms the optical pathway in the prism material changes accordingly for the different wavelengths and therefore the amount of dispersion (chirp) can be controlled. Without optimizing and characterizing the magnitude of the introduced chirp we were able to achieve a nearly exclusive excitation of $v_2/v_{2'}$. This is very clearly demonstrated with the transient shown in panel (B) of Fig 3.

Even much better results can be achieved if a more systematic change of the phases of the exciting laser pulses is performed[30]. In the experiment described above we were able to influence basically the linear chirp of the lasers. Using a pulse-shaper as suggested by Weiner et al.[59], the phase shape of the laser pulses can be influenced in a much more distinguished way than described above. Applying a feedback-optimized technique as suggested by Judson and Rabitz[60] and recently verified by Assion et al.[61] one is able to perform optimal control of the mode excitation in complicated molecular systems. The basic idea is to overcome statistics by a state-selective chemistry. Bonds have to be broken and formed selectively. The main problem here is the intramolecular vibrational energy redistribution (IVR) where the energy deposited in certain bonds is redistributed over all the other modes of the molecules on a femto- to picosecond time scale. Bond-selective excitation may be achieved by manipulating the dynamics of a system by means of a coherent laser field such that the system is steered towards a desired state or reaction channel. As shown above ultrashort laser pulses are spectrally broad and are capable of coherently exciting more than one normal mode. If the phases of these modes are correctly chosen, the enhancement of certain normal modes or the preparation of local modes should be possible. Feedback controlled shaping of ultrashort pulses seems to be the most general scheme for coherent control. If we are able to control the excitation of normal modes, we also should be able to excite normal modes in such a way that certain bonds are efficiently excited; this scheme would be of great interest for a possible reaction control. Very recently such experiments have been set into realization[30].

3.4 β-carotene: Population Dynamics in Vibrational Modes during Non-Born-Oppenheimer Processes

In a third experiment one utilises the capability of the CARS process to interrogate individual normal modes as has been shown by the two experiments presented above for exploring the influence of nuclear dynamics on the process of internal conversion (IC). Ultrafast intramolecular non-radiative processes such as internal conversion (IC) play a crucial role in the mechanism of photochemical[62,63] and photobiological processes such as vision[64] and photosynthesis and underline the general concepts associated with molecular electronics[65]. Of special interest is the influence of different normal modes on the rate of internal conversion. The capability of the CARS process to interrogate individual normal modes was utilised in this work for exploring the influence of nuclear dynamics on the process of IC, by placing the CARS process in a *pump-probe* scheme, where it plays the role of a mode selective probe.

This selectivity is utilised for interrogating the population flow in normal modes of β-carotene, a molecule which plays a primary role in photosynthesis, subsequent to the S_1/S_0 IC using the experimental scheme shown in the left side of Fig 4. An initial *pump* laser (λ_{IP} = 400 nm) transfers population to the first optically accessible S_2 state. The subsequent S_1/S_0 IC, vibrational cooling and internal vibrational energy redistribution (IVR) is interrogated mode-selectively via a time-variable CARS process consisting of two *pump* lasers (1 and 3 in Fig 4, λ_{pu}= 510 nm) also utilizing the $S_2 \leftarrow S_0$ optical transition and a Stokes laser (2 in Fig 4, λ_S = 530-550 nm) which allows for the CARS process to be tuned to different normal modes ($\Delta\tilde{\nu}$) in the S_0 state. Lasers 1-3 generate the CARS signal (4, in Fig. 4) which is monitored as a function of the delay time, (Δt) between the initial *pump* laser IP and the CARS process (see right side of Fig. 4). The experimental scheme corresponds to probing of an electronic ground state bleach induced by the population transfer into the S_2-state via the initial *pump* pulse IP.
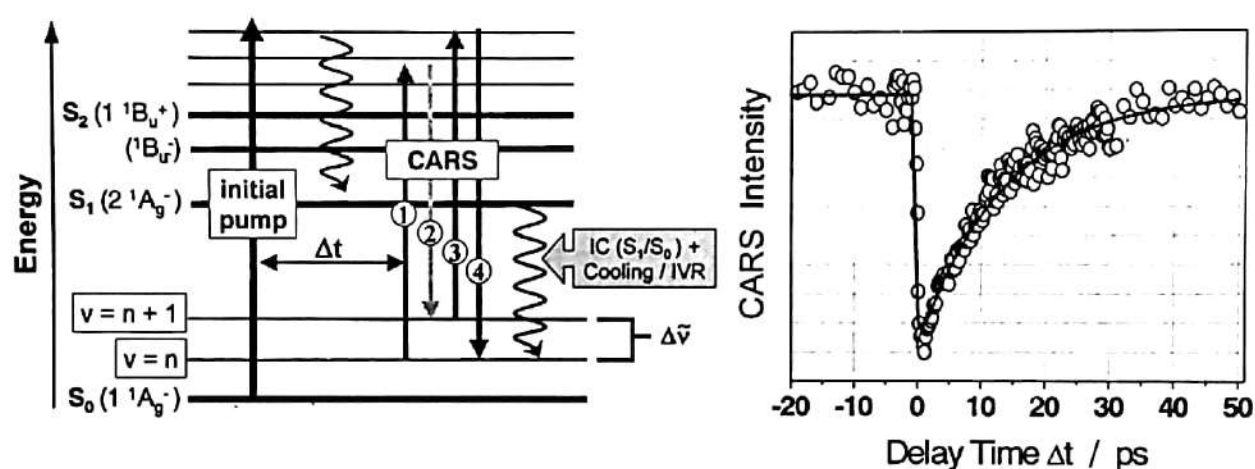

Figure 4 Left side: Schematic energy diagram of all-trans-β-carotene illustrating the excitation by means of an initial pump laser and a mode-selective interrogation via a time-variable CARS process by tuning the CARS lasers to be resonant with a Raman transition in the S_0 state. Right side: intensity of the CARS signal plotted as a function of the delay time Δt, between the *initial pump* laser and the CARS process.

At Δt = 0, the initial *pump* laser and the CARS process interact simultaneously with the system. The transfer of population to the S_2 state and the corresponding bleach of the electronic ground state induced by the initial *pump* laser leads to a drop in the CARS intensity due to the depletion of ground state molecules available for the CARS scattering process. For positive delay times a recovery of the CARS intensity takes place with increasing delay time. This corresponds to a repopulation of the vibrational states that are interrogated by means of the CARS process through the S_1/S_0 IC and subsequent vibrational relaxation. The repopulation of the normal modes in the ground state can be attributed solely to the non-radiative process of IC since the $S_0 \leftarrow S_1$ transition is optically forbidden which rules out fluorescence. The repopulation of the vibrational states in the electronic ground state can be characterized with a mono-exponential recovery time-constant, τ convoluted with a Gaussian profile representing the temporal response function.

By tuning the CARS process to be resonant with different Raman modes of β-carotene in the S_0 state, the recovery time τ and with this, the flow of population into the different normal modes during the S_1/S_0 IC can be monitored. The experimental τ values determined for five different spectral positions of the CARS signal corresponding to the Raman shift of five vibrational modes of β-carotene in the S_0 state

are summarized in Table 2 and the values for τ clearly show that the population flow from the S_1 state into the electronic ground state is not uniform for the normal modes that were interrogated. The results show that different recovery times, into the electronic ground state where recorded when the CARS process was tuned to $\Delta\tilde{v}$ = 1524 cm^{-1} (τ = 8.46 ps) and $\Delta\tilde{v}$ = 1269 cm^{-1} (τ = 13.40 ps), which correspond to the normal modes with a strong contribution in the C-C double bond symmetric stretching and C-H in plane bending, respectively. All other normal modes show values that lie in between the above mentioned recovery times. Overall, the results show different recovery times for the different normal modes in the electronic ground state after the S_1/S_0 internal conversion.

Table 2. Recovery time τ for different normal modes of β-carotene dissolved in dichloromethane

Wavenumber / cm^{-1}	Recovery Time τ / ps	Characteristic Motion
1524	8.46	C=C symmetric stretch
1269	13.40	C-H in plane bending with C-C stretch
1157	8.92	C-C symmetric stretch
1006	9.13	methyl to chain stretch
872	10.90	C=C-C bending

The mechanism, with which the CARS process can act as a selective probe of the population within the vibrational states of a specific normal mode has its foundation in the strong enhancement of the CARS intensity in the case that the energy difference between the *pump* and Stokes laser is resonant to a Raman transition. The lack of a Raman resonance forces the CARS process to go through a virtual intermediate state, making the generation of the CARS signal out of the initial state (v=n) through the interaction with lasers 1 - 3 extremely ineffective. Therefore the Raman resonance and not the electronic resonance of the *pump* laser is the most influential when considering the CARS signal intensity from a particular vibrational state in the total signal. As long as the energy difference between excited vibrational state (v = n and v = n + 1) is still resonant to the energy difference of the *pump* and *Stokes* laser, the Raman resonance will primarily determine the signal intensity while the lack of a Raman resonance will lead to a much weaker signal. With this, the Raman resonance can be seen as an intensity filter for the CARS signal.

With this information, it is possible to gain direct insight into the exact mechanism of the S_1/S_0 IC with respect to the nuclear dynamics involved in this electronic transition. The recovery time of τ = 8.46 ps for the normal mode at 1524 cm^{-1}, which is dominated by a large amplitude motion along the C=C symmetric stretch in the polyene backbone of β-carotene, is clearly the fastest recovery time. From this, it can be postulated that the fastest time constant of population recovery in the electronic ground state for this vibrational mode is direct experimental evidence that this mode acts as the primary accepting mode for population flow in the S_1/S_0 internal conversion. The fast recovery time for this mode in comparison to the recovery times measured for all other vibrational modes, shows that the population flow between the S_1 and S_0 potential energy surface is primarily funneled through this form of nuclear motion and then spreads out over the other normal modes of the energetically lower lying potential energy surface via internal vibrational energy redistribution and cooling. Therefore the slower recovery times measured for the normal modes with τ = 9.13 to 13.40 ps will be determined by (*i*) the time scale with which the vibrational modes of the C=C symmetric stretch mode are populated by means of population transfer from the S_1 state and subsequent cooling within the C=C symmetric stretch mode and,

(*ii*) the following internal vibrational energy redistribution out of the excited vibrational states of the C=C symmetric stretch into the vibrational states of other modes with subsequent cooling in these modes.

4 CONCLUSION

Femtosecond time-resolved CARS spectroscopy is a technique that utilizes the broad spectral bandwidths associated with femtosecond laser pulses in order to prepare and monitor coherent states of the sample in its excited or electronic ground state, respectively. The time evolution of wave packets prepared by such methods gives information on the dynamics of molecular vibrations. In this paper we have focused on three different experimental works performed in our laboratories.

Firstly we reported on femtosecond time-resolved CARS measurements on magnesium octaethylporphyrin dissolved in dichloromethane. In order to supress the non-Raman resonant background special polarization geometries of the fs pulses and the coherently scattered CARS signal were employed. Fast beating patterns in the 100 to 200 fs range were observed between several porphyrin normal modes with T_2 relaxation times of ca. 700 fs.

In a second experiment, we reported on fs time-resolved CARS measurements on diacetylene (polydiacetylene), which were performed in order to selectively excite coherent vibrational motions in the electronic ground state of these polyatomic molecules. The CARS laser wavenumbers were chosen such that electronic as well as Raman resonances were met. The control of mode excitation was performed by changing the phase shape of the exciting laser pulses in a non-systematic way. By doing so we were able to focus the excitation into the ν_2 mode.

In a third experiment the capability of the CARS process has been utilised to interrogate individual normal modes as has been shown in the first two examples for exploring the influence of nuclear dynamics on the process of internal conversion (IC), by placing the CARS process in a *pump-probe* scheme, where it plays the role of a mode selective probe. This selectivity is utilised for interrogating the population flow in normal modes of β-carotene, a molecule which plays a primary role in photosynthesis, subsequent to the S_1/S_0 IC. It could be shown that the C=C-stretching motion acts as a primary acceptor mode in the S_1/S_0 IC, i.e. the population flow during the transition from the S_1 to the S_0 potential energy surface (PES) is funneled predominately into this normal mode.

Acknowledgment

References

1 Manz J, Wöste L, *Femtosecond Chemistry*. (VCH, Weinheim), 1995.
2 Chergui M, *Femtochemistry*. (World Scientific, Singapore) 1996.
3 Kaiser W, *Ultrashort Laser Pulses*. (Topics in Applied Physics; Springer, Berlin) 1988.
4 Zewail A H, *J Phys Chem*, 97 (1993) 12427.
5 Zewail A H, *Femtochemistry: Ultrafast Dynamics of the Chemical Bond Vol. I+II*. (World Scientific, Singapore), 1994.
6 Sundström V, *Femtochemistry and Femtobiology: Ultrafast Reaction Dynamics at Atomic-Scale Resolution. Nobel Symposium 101*. (Imperial College Press, London), 1996.

7   Baumert T, Engel V, Meier C, Gerber G, *Chem Phys Lett* 200 (1992) 488.
8   Baumert T, Thalweiser R, Gerber G, *Chem Phys Lett* 209 (1993) 29-34.
9   Schreiber E, *Proc Int Conf Lasers '94*. (STS Press, McLean) 1995, p. 490.
10   Vivie-Riedle R D, Manz J, Meyer W, Reischl B, Rutz S, Schreiber E, Wöste L, *J Phys Chem,* 100 (1996) 7789.
11   Bardeen, C J, Wang, Q, Shank C V, *Ultrafast Phenomena*. (Springr, Berlin), 1996, p 203.
12   Lian T, Bromberg S E, Asplund M C, Yang H, Harris C B, *J Phys Chem,* 100 (1996) 11994.
13   Anfinrud P, de Vivie-Riedle R, Engel V, *Proc Natl Acad Sci USA,* 96 (1999) 8328.
14   Pausch R, Heid M, Chen T, Kiefer, W, Schwoerer H, *J Chem Phys,* 110 (1999) 9560.
15   Leonhardt R, Holzapfel W, Zinth W, Kaiser W, *Chem Phys Lett,* 133 (1987) 373.
16   Zinth W, Leonhardt R, Holzapfel W, Kaiser W *IEEE J Quant Electr,* 24 (1988) 455.
17   Bron W E, Juhasz T, Mehta S, *Phys Rev Lett,* 62 (1989) 1655.
18   Fickenscher M, Laubereau A, *J Raman Spectrosc,* 21 (1990) 857.
19   Okamoto H, Yoshihara K, *J Opt Soc Am B,* 7 (1990) 1702.
20   Okamoto H, Yoshihara K, *Chem Phys Lett,* 177 (1991) 568.
21   Joo T, Dugan M A, Albrecht A C, *Chem Phys Lett,* 177 (1991) 4.
22   Fickenscher M, Purucker H G, Laubereau A, *Chem Phys Lett,* 191 (1992) 182.
23   Okamoto H, Inaba R, Yoshihara K, Tasumi M, *Chem Phys Lett,* 202 (1993) 161.
24   Yang T S, Zhang R, Myers A B, *J Chem Phys,* 100 (1994) 8573.
25   Hayden C C, Chandler D W, *J Chem Phys,* 103 (1995) 10465.
26   Lang T, Kompa K L, Motzkus M, *Chem Phys Lett,* 310 (1999) 65.
27   Chen T, Vierheilig A, Waltner P, Kiefer W, Materny A, *Chem Phys Lett,* 325 (2000) 176.
28   Chen T, Vierheilig A, Waltner P, Heid M, Kiefer W, Materny A, *Chem Phys Lett,* 326 (2000) 375.
29   Chen T, Vierheilig A, Kiefer W, Materny A, *PhysChemChemPhys,* 3 (2001) 5408.
30   Zeidler D, Frey S, Wohlleben W, Motzkus M, Busch F, Chen T, Kiefer W, Materny A, *J Chem Phys,* 116 (2002) 5231.
31. Siebert T, Schmitt M, Vierheilig A, Flachenecker G, Materny A, Kiefer W, *J Raman Spectrosc,* 31 (2000) 25.
32   Heid M, Chen T, Schmitt U, Kiefer W, *Chem Phys Lett,* 334 (2001) 119.
33   Heid M, Schlücker S, Schmitt U, Chen T, Schweitzer-Stenner R, Engel V, Kiefer W, *J Raman Spectrosc,* 32(9) (2001) 771.
34   Heid M, Chen T, Materny A, Kiefer W, *Proceedings of the International Conference on Lasers '00*. (STS Press, McLean), 2001, p 181.
35   Siebert T, Schmitt M, Engel V, Materny A, Kiefer W, *J Am Chem Soc,* 124 (2002) 6242.
36   Siebert T, Maksmenka R, Materny A, Engel V, Kiefer W, Schmitt M, *J Raman Spectrosc,* to be published.
37   Schmitt M, Knopp G, Materny A, Kiefer W, *Chem Phys Lett,* 270 (1997) 9.
38   Schmitt M, Knopp G, Materny A, Kiefer W, *Chem Phys Lett,* 280 (1997) 339.
39   Meyer S, Schmitt M, Materny A, Kiefer W, Engel V, *Chem Phys Lett,* 281 (1997) 332.
40   Meyer S, Schmitt M, Materny A, Kiefer W, Engel V, *Chem Phys Lett,* 287 (1998) 753.
41   Schmitt M, Knopp G, Materny A, Kiefer W, *J Phys Chem A,* 102 (1998) 4059.
42   Rubner O, Schmitt M, Knopp G, Materny A, Kiefer W, Engel V, *J Phys Chem A,* 102 (1998) 9734.
43   Chen T, Engel V, Heid M, Kiefer W, Knopp G, Materny A, Meyer S, Pausch R, Schmitt M, Schwoerer H, Siebert T, *Vib Spectrosc,* 19 (1999) 23.
44   Chen T, Dietz H, Engel V, Heid M, Kiefer W, Knopp G, Materny A, Meyer S, Pausch R, Schmitt M, Schwoerer H, Siebert T, *SPIE Proc,* 3733 (1999) 2.
45   Chen T, Engel V, Heid M, Kiefer W, Knopp G, Materny A, Meyer S, Pausch R, Schmitt M, Schwoerer H, Siebert T, *J Mol Struct,* 480-481 (1999) 33.
46   Meyer S, Schmitt M, Materny A, Kiefer W, Engel V, *Chem Phys Lett,* 301 (1999) 248.
47   Siebert T, Schmitt M, Michelis T, Materny A, Kiefer W, *J Raman Spectrosc,* 30 (1999) 807.
48   Knopp G, Schmitt M, Materny A, Kiefer W, *J Phys Chem,* 101 (1997) 4852.
49   Maeda S, Kamisuki T, Adachi Y, *Advances in Non-Linear Spectroscopy*. (Wiley & Sons, Chichester), 1988, p 253.
50   Wegner G, *Z Naturforsch,* 24B (1969) 824.
51   Materny A, Kiefer W, *Macromol,* 25 (1992) 5074.

52   Kiefer W, Schmitt M, Siebert T, Heid M, Materny A, Grabtchikov A S, Orlovich V, *Proceedings of XVIIIth International Conference on Raman Spectroscopy.* (John Wiley & Sons, Chichester), 2002, p 7.
53   Li W, Purucker H-G, Laubereau A *Opt Commun,* 94 (1992) 300.
54   Nissum M, Funk M J, Kiefer W, *J Raman Spectrosc,* 30 (1999) 605.
55   Li X Y, Czernuszewicz R S, Kincaid J R, Su Y O, Spiro T G, *J Phys Chem,* 94 (1990) 31.
56   Zewail A H, Bernstein R, *Chem Eng News,* 66 (1988) 24.
57   Pham T A, Daunois A, Merle J-C, Le Moigne J, Bigot, J Y, *Phys Rev Lett,* 74 (1995) 904.
58   Kobayashi T, Yoshizama M, Stamm U, Taiji M, Hasegawa M, *J Opt Soc Am,* 7 (1990) 1558.
59   Weiner A M, Leaird D E, Patel J S, Wullert J R II, *Opt Lett,* 15 (1992) 326.
60   Judson R S, Rabitz H, *Phys Rev Lett,* 68 (1992) 1500.
61   Assion A, Baumert T, Bergt M, Brixner T, Kiefer B, Seyfried V, Strehle M, Gerber G, *Science,* 282 (1998) 919.
62   Freed K F, *Radiationless Processes in Molecules and Condensed Phase.* (Springer, Berlin), 1976, p 23.
63   Stock G, Domcke W, *Adv Chem Phys,* 100 (1997) 1.
64   Schoenlein R W, Peteanu L A, Mathies R A, Shank C V, *Science,* 254 (1991) 412.
65   Jortner J, Ratner M A, *Molecular Electronics,* (IUPAC, Blackwell, Oxford), 1997.